Spin Filter, Spin Amplifier and Other Spintronic Applications in Graphene Nanodisks

Motohiko Ezawa
Department of Applied Physics, University of Tokyo, Hongo 7-3-1, 113-8656, Japan

Graphene nanodisk is a graphene derivative with a closed edge. The trigonal zigzag nanodisk with size N has N-fold degenerated zero-energy states. A nanodisk can be interpletted as a quantum dot with an internal degree of freedom. The grand state of nanodisk has been argued to be a quasi-ferromagnet, which is a ferromagnetic-like states with a finite but very long life time. We investigate the spin-filter effects in the system made of nanodisks and leads based on the master equation. The finite-size effect on spin filter is intriguing due to a reaction from the polarization of incoming current to a quasi-ferromagnet. Analyzing the relaxation process with the use of the Landau-Lifshitz-Gilbert equation, we explore the response to four types of incoming currents, namely, unpolarized current, perfectly polarized current, partially polarized current and pulse polarized current. We propose some applications for spintronics, such as spin memory, spin amplifier, spin valve, spin-field-effect transistor and spin diode.

I. INTRODUCTION

The study of spin-dependent transport phenomena has recently attracted much attention.[1,2] It has opened the way for the field of spintronics,[3,4,5,6,7] literally spin electronics, where new device functionalities exploit both the charge and spin degrees of freedom. There are various approaches in this sphere. For instance, the use of a quantum-dot setup[8,9] has been proposed, which can be operated either as a spin filter to produce spin-polarized currents or as a device to detect and manipulate spin states. Spintronics in graphene has also been proposed[10,11,12] recently. In the following we address this issue in a new type of materials, graphene nanodisks.[13,14,15,16,17]

Graphene nanostructure[18,19,20] such as graphene nanoribbons[21,22,23,24,25,26,27,28,29,30] and graphene nanodisks[13,14,15,16,17] could be basic components of future nanoelectronic and spintronic devices. Graphene nanodisks are nanometer-scale disk-like materials which have closed edges. They are constructed by connecting several benzenes, some of which have already been manufactured by soft-landing mass spectrometry.[27,31,32] There are varieties of nanodisks, among which zigzag trigonal nanodisks with size N are prominent because they have N-fold degenerated zero-energy states. We have already shown[14] that spins make a ferromagnetic order and that the relaxation time is finite but quite large even if the size N is very small. We refer to this property as quasi-ferromagnet. Furthermore we have argued[17] that a nanodisk behaves as if it were a quantum dot with an internal degree of freedom, where the conductance exhibits a peculiar series of Coulomb blockade peaks.

In this paper we make an investigation of the spin current in the zero-energy sector of the trigonal zigzag nanodisk. We first analyze how the spin of a nanodisk filters the spin of the current by assuming that the nanodisk is a rigid ferromagnet. The fact that the direct and exchange Coulomb interactions are of the same of magnitude plays an important role. However the nanodisk is not a rigid ferromagnet but a quasi-ferromagnet. Hence an intriguing reaction phenomenon occurs: Namely, the spin of the nanodisk can be controlled by the spin of the current. Using these properties we propose some applications for spintronic devices, such as spin memory, spin amplifier, spin valve, spin-field-effect transistor and spin diode.

This paper is organized as follows. In Sec.II, we summarize the basic notion of the nanodisk. The low-energy physics is described by electrons in the N-fold degenerated zero-energy sector, which form a quasi-ferromagnet due to a large exchange interaction. In Sec.III, we investigate the spin-filter effects based on the master equation. In Sec.IV, we analyze the reaction to the spin of the nanodisk from the spin of electrons in the current. We discuss the relaxation process using the Landau-Lifshitz-Gilbert equation. In Sec.V, we propose various spintronic devices and explore their properties.

II. NANODISK QUASI-FERROMAGNETS

A. Zero-Energy Sector

Graphene nanodisks are graphene derivatives which have closed edges. The Hamiltonian is defined by

$$H = \sum_i \varepsilon_i c_i^\dagger c_i + \sum_{\langle i,j\rangle} t_{ij} c_i^\dagger c_j, \tag{2.1}$$

where ε_i is the site energy, t_{ij} is the transfer energy, and $c_i^\dagger$ is the creation operator of the π electron at the site i. The summation is taken over all nearest neighboring sites $\langle i,j\rangle$. Owing to their homogeneous geometrical configuration, we may take constant values for these energies, $\varepsilon_i = \varepsilon_{\rm F}$ and $t_{ij} = t \approx 2.70$eV.

We have searched for zero-energy states or equivalently metallic states in graphene nanodisks with various sizes and shapes.[14] The emergence of zero-energy states is surprisingly rare. Among typical nanodisks, only trigonal zigzag nanodisks have degenerate zero-energy states and show metallic ferromagnetism, where the degeneracy can be controlled arbitrarily by designing the size.

Trigonal zigzag nanodisks are specified by the size parameter N as in Fig.1(a). The size-N nanodisk has N-fold degenerated zero-energy states,[14] where the gap energy is as large as a few eV. Hence it is a good approximation to investigate the

electron-electron interaction physics only in the zero-energy sector, by projecting the system to the subspace made of those zero-energy states. The zero-energy sector consists of N orthonormal states $|f_\alpha\rangle$, $\alpha = 1, 2, \cdots, N$, together with the SU(N) symmetry. We can expand the wave function of the state $|f_\alpha\rangle$,

$$f_\alpha(\boldsymbol{x}) = \sum_i \omega_i^\alpha \varphi_i(\boldsymbol{x}), \tag{2.2}$$

in terms of the Wannier function $\varphi_i(\boldsymbol{x})$ localized at the site i. The amplitude ω_i^α is calculable by diagonalizing the Hamiltonian (2.1).

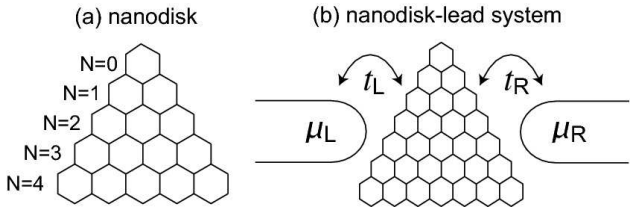

FIG. 1: (a) Trigonal zigzag nanodisks. The size parameter N is defined in this way. The number of carbon atoms is given by $N_C = N^2 + 6N + 6$. (b) The nanodisk-lead system. The nanodisk with $N = 7$ is connected to the right and left leads by tunneling coupling t_R and t_L. The chemical potential is μ_R or μ_L at each lead.

B. Quasi-Ferromagnets

We include the Coulomb interaction between electrons in the zero-energy sector.[17] It is straightforward to rewrite the Coulomb Hamiltonian as

$$\begin{aligned} H_D^{\text{eff}} = & \sum_{\alpha \geq \beta} U_{\alpha\beta} n(\alpha) n(\beta) \\ & - \frac{1}{2} \sum_{\alpha > \beta} J_{\alpha\beta} [4\boldsymbol{S}(\alpha) \cdot \boldsymbol{S}(\beta) + n(\alpha) n(\beta)], \end{aligned} \tag{2.3}$$

where $U_{\alpha\beta}$ and $J_{\alpha\beta}$ are the Coulomb energy and the exchange energy between electrons in the states $|f_\alpha\rangle$ and $|f_\beta\rangle$. Here, $n(\alpha)$ is the number operator and $\boldsymbol{S}(\alpha)$ is the spin operator,

$$n(\alpha) = d_\sigma^\dagger(\alpha) d_\sigma(\alpha), \tag{2.4a}$$

$$\boldsymbol{S}(\alpha) = \frac{1}{2} d_\sigma^\dagger(\alpha) \boldsymbol{\tau}_{\sigma\sigma'} d_{\sigma'}(\alpha), \tag{2.4b}$$

with $d_\sigma(\alpha)$ the annihilation operator of electron with spin $\sigma = \uparrow, \downarrow$ in the state $|f_\alpha\rangle$: $\boldsymbol{\tau}$ is the Pauli matrix.

The remarkable feature is that there exists a large overlap between the wave functions $f_\alpha(\boldsymbol{x})$ and $f_\beta(\boldsymbol{x})$, $\alpha \neq \beta$, since the state $|f_\alpha\rangle$ is an ensemble of sites as in (2.2) and identical sites are included in $|f_\alpha\rangle$ and $|f_\beta\rangle$. Consequently, the dominant contributions come from the on-site Coulomb terms not only for the Coulomb energy but also for the exchange energy: Indeed, it follows that $U_{\alpha\beta} = J_{\alpha\beta}$ in the on-site approximation. We thus obtain

$$U_{\alpha\beta} \simeq J_{\alpha\beta} \simeq U \sum_i (\omega_i^\alpha \omega_i^\beta)^2, \tag{2.5}$$

where

$$U \equiv \sum_{i,j} \int d^3x d^3y \; \varphi_i^*(\boldsymbol{x}) \varphi_i(\boldsymbol{x}) V(\boldsymbol{x} - \boldsymbol{y}) \varphi_j^*(\boldsymbol{y}) \varphi_j(\boldsymbol{y}) \tag{2.6}$$

with the Coulomb potential $V(\boldsymbol{x} - \boldsymbol{y})$. The Coulomb energy U is of the order of 1eV because the lattice spacing of the carbon atoms is ~ 1Å in graphene.

Since the exchange energy $J_{\alpha\beta}$ is as large as the Coulomb energy $U_{\alpha\beta}$, the spin stiffness $J_{\alpha\beta}$ is quite large. Furthermore, we have checked[17] numerically that all $J_{\alpha\beta}$ are of the same order of magnitude for any pair of α and β, implying that the SU(N) symmetry is broken but not so strongly in the Hamiltonian (2.3). It is a good approximation to start with the exact SU(N) symmetry. Then, the zero-energy sector is described by the SU(N) Heisenberg-Hubbard model,

$$\begin{aligned} H_D = & - J \sum_{\alpha \neq \beta} \boldsymbol{S}(\alpha) \cdot \boldsymbol{S}(\beta) \\ & + \left(\frac{U}{2} - \frac{J}{4} \right) \sum_{\alpha \neq \beta} n(\alpha) n(\beta) + U \sum_\alpha n(\alpha), \end{aligned} \tag{2.7}$$

with $J \approx U$. We rewrite H_D as

$$\begin{aligned} H_D = & - J \left[S_{\text{tot}}^2 - \sum_\alpha \boldsymbol{S}^2(\alpha) \right] + \left(\frac{U}{2} - \frac{J}{4} \right) n_{\text{tot}}^2 \\ & + \left(\frac{U}{2} + \frac{J}{4} \right) \sum_\alpha n(\alpha) \\ = & - J S_{\text{tot}}^2 + \left(\frac{U}{2} - \frac{J}{4} \right) n_{\text{tot}}^2 + \left(\frac{U}{2} + J \right) n_{\text{tot}} \end{aligned} \tag{2.8}$$

in terms of the total spin,

$$\boldsymbol{S}_{\text{tot}} = \sum_\alpha \boldsymbol{S}(\alpha), \tag{2.9}$$

and the total electron number,

$$n_{\text{tot}} = \sum_\alpha n(\alpha). \tag{2.10}$$

At the half-filling, the eigenstate of the Hamiltonian H_D is labeled as $|s\rangle = |n_{\text{tot}}, l, m\rangle$, where l is the total spin-angular momentum and m is its z-component. Based on this Hamiltonian we have shown[14] that the relaxation time of the ferromagnetic-like spin polarization is quite large even if the size of trigonal zigzag nanodisks is quite small. Such a nanodisk may be called a quasi-ferromagnet. We refer to the total spin $\boldsymbol{S}_{\text{tot}}$ of a nanodisk as the nanodisk spin.

C. Nanodisk-Lead System

We consider a system made of a nanodisk connected by two metallic leads [Fig.1(b)]. The model Hamiltonian is given by

$$H = H_L + H_{TL} + H_{TR} + H_D, \tag{2.11}$$

where $H_{\rm D}$ is the Hamiltonian (2.7) of a nanodisk, and $H_{\rm L}$ is the lead Hamiltonian

$$H_{\rm L}=\sum_{k\sigma}\varepsilon\left(k\right)\left(c_{k\sigma}^{\rm L\dagger}c_{k\sigma}^{\rm L}+c_{k\sigma}^{\rm R\dagger}c_{k\sigma}^{\rm R}\right). \tag{2.12}$$

The Hamiltonian $H_{\rm L}$ describes a noninteracting electron gas in the leads with $\varepsilon\left(k\right)=\hbar^2\boldsymbol{k}^2/2m$, while $H_{\rm TL}$ and $H_{\rm TR}$ are the transfer Hamiltonian between the left (L) and right (R) leads and the nanodisk, respectively,

$$H_{\rm TL}=t_{\rm L}\sum_{k\sigma}\sum_{\alpha}\left(c_{k\sigma}^{\rm L\dagger}d_{\sigma}(\alpha)+d_{\sigma}^{\dagger}(\alpha)c_{k\sigma}^{\rm L}\right), \tag{2.13a}$$

$$H_{\rm TR}=t_{\rm R}\sum_{k\sigma}\sum_{\alpha}\left(c_{k\sigma}^{\rm R\dagger}d_{\sigma}(\alpha)+d_{\sigma}^{\dagger}(\alpha)c_{k\sigma}^{\rm R}\right), \tag{2.13b}$$

with t_χ the tunneling coupling constant: We have assumed that the spin does not flip in the tunneling process.

The nanodisk-lead system looks similar to that of the N-dot system.[33] However, there exists a crucial difference. On one hand, in the ordinary N-dot system, an electron hops from one dot to another dot. On the other hand, in our nanodisk system, the index α of the Hamiltonian runs over the N-fold degenerate states and not over the sites. According to the Hamiltonian (2.13), an electron does not hop from one state to another state. Hence, it is more appropriate to regard our nanodisk as a one-dot system with an internal degree of freedom.

III. SPIN FILTER

The aim of this paper is to investigate a nanodisk as a spin filter[38] based on the Hamiltonian (2.11). The setup we consider is a lead-nanodisk-lead system [Fig.1(b)], where an electron makes a tunnelling from the left lead to the nanodisk and then to the right lead. We investigate how the electron spin is affected by the nanodisk spin during the transport process.

The dynamics of the nanodisk system is described by the master equation,

$$\frac{\partial\rho\left(s\right)}{\partial t}=\sum_{s'}\left[W\left(s,s'\right)\rho\left(s'\right)-W\left(s',s\right)\rho\left(s\right)\right], \tag{3.1}$$

where $\rho\left(s\right)$ represents the probability to find the system in the state $|s\rangle=|n_{\rm tot},l,m\rangle$, and $W\left(s',s\right)$ is the transition rate between the states $|s\rangle$ and $|s'\rangle$. The master equation describes a stochastic evolution in the space spanned by the states $|s\rangle$. Jumps between different states are assumed to be Markovian. The stationary solution is given by the detailed balance condition $\partial\rho/\partial t=0$.

Since the Hamiltonian $H_{\rm D}$ only depends on $S_{\rm tot}^2$, the probability $\rho(s)$ has no dependence on the spin component m. Then it is convenient to do a sum over m,

$$\overline{\rho}\left(\overline{s}\right)=\sum_{m}\rho\left(s\right) \tag{3.2}$$

with $|\overline{s}\rangle=|n_{\rm tot},l\rangle$. The master equation is rewritten as

$$\frac{\partial\overline{\rho}\left(\overline{s}\right)}{\partial t}=\sum_{s'}\left[W\left(\overline{s},\overline{s}'\right)\overline{\rho}\left(\overline{s}'\right)-W\left(\overline{s}',\overline{s}\right)\overline{\rho}\left(\overline{s}\right)\right]. \tag{3.3}$$

In the following we denote $\overline{\rho}\left(\overline{s}\right)$ as $\rho\left(s\right)$ for simplicity.

In this paper we consider the small coupling limit, $t_\chi\ll J$, χ =L, R, where the dominant process is the sequential tunneling: It is of the order of $|t_\chi|^2$, while the cotunneling process of the order of $|t_\chi|^4$.

In the sequential-tunneling regime the transition rate, $W=W_{\rm L}+W_{\rm R}$, is obtained by the Fermi's golden rule,[8,34,35]

$$\begin{aligned}W_\chi\left(s',s\right)=&\Gamma_\chi f_\chi\left(\Delta_{s's}\right)\delta_{n',n+1}\\&+\Gamma_\chi\left[1-f_\chi\left(\Delta_{s's}\right)\right]\delta_{n',n-1}.\end{aligned} \tag{3.4}$$

Let us explain notations. First,

$$f_\chi\left(\varepsilon\right)=\left\{1+\exp\left[\left(\varepsilon-\mu_\chi\right)/k_{\rm B}T\right]\right\}^{-1} \tag{3.5}$$

is the Fermi function at temperature T, with μ_χ the chemical potential at the right or left lead, χ =R,L. We set

$$\mu_{\rm L}=\mu+\Delta\mu,\quad \mu_{\rm R}=\mu-\Delta\mu. \tag{3.6}$$

Second, $\Delta_{s's}$ is the energy difference between the two states $|s'\rangle$ and $|s\rangle$,

$$\Delta_{s's}=E_{s'}-E_s. \tag{3.7}$$

Third,

$$\Gamma_\chi=2\pi\nu\left|A_{\chi,ss'}^{\sigma}\right|^2 \tag{3.8}$$

is the tunneling rate through the right or left lead, where $\nu=\sum_k\delta\left(\varepsilon_{\rm F}-\varepsilon_k\right)$ is the density of states at the Fermi level $\varepsilon_{\rm F}$ in the leads, which is a constant, and

$$A_{\chi,ss'}^{\sigma}=t_\chi\sum_{\alpha}\left\langle s'\right|d_{\alpha\sigma}\left|s\right\rangle. \tag{3.9}$$

It follows that the tunneling rate Γ_χ is a constant for the states $|s\rangle$ and $|s'\rangle$ connected by a Markov step, and zero otherwise.

The current through the nanodisk can be written as

$$I_\sigma=\sum_{s,s'}\left[W_{\rm R}\left(s',s\right)\rho\left(s\right)-W_{\rm R}\left(s,s'\right)\rho\left(s'\right)\right], \tag{3.10}$$

where $\sum_{s,s'}$ runs over the states $|s\rangle$ and $|s'\rangle$ such that $\langle s'|\,d_{\alpha\sigma}\,|s\rangle\neq0$. Thus the current I_σ depend on the spin configuration of electrons in the nanodisk.

We have argued that the nanodisk is a quasi-ferromagnet. For the sake of simplicity, we start with the simplification that the ground state is a ferromagnet with polarized up-spins. When the transition interaction is small enough, a single electron tunnels at once, namely, the electron number in the nanodisk increases or decreases by one, $n'_{\rm tot}=n_{\rm tot}\pm1$. First of all, we notice that, when $n'_{\rm tot}=n_{\rm tot}+1$, the tunneling of spin-up electrons is blocked by the Pauli's exclusion principle. The Markov chain of spin configurations contain only a finite number of states. For instance it is 9 in the case of $N=5$ nanodisk. We number them as indicated in Fig.2.

We calculate the energy E_s of various states $|s\rangle=|n_{\rm tot},l\rangle$ in this chain. According to the above numbering convention (Fig.2), they are

$$\begin{aligned}E_1=&E_{N,N/2},\quad E_2=E_{N-1,(N-1)/2},\quad E_3=E_{N,N/2-1},\\E_4=&E_{N-1,(N-3)/2},\quad E_5=E_{N+1,(N-1)/2},\quad\cdots.\end{aligned} \tag{3.11}$$

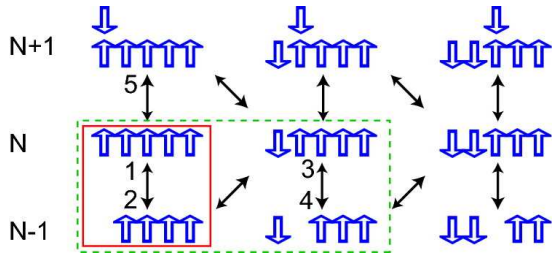

FIG. 2: Markov chain of spin configurations in the $N = 5$ nanodisk. An arrow ($\updownarrow$) indicates each Markov step between two states with different spin configurations. The region surrounded by red solid lines shows the most dominant process for spin-polarized current. In this approximation there is no down-spin polarized current. The region surrounded by green dotted lines yields the next dominant contribution, which allows a down-spin polarized current as well.

Based on the effective Hamiltonian (2.8) they are calculated as follows,

$$E_1 = \frac{U-J}{2}N^2 + \frac{U+J}{2}N \approx UN, \tag{3.12a}$$

$$E_2 = \frac{U-J}{2}(N-1)^2 + \frac{U+J}{2}(N-1) \approx U(N-1), \tag{3.12b}$$

$$E_3 = \frac{U-J}{2}N^2 + \frac{U+3J}{2}N \approx 2UN, \tag{3.12c}$$

$$E_4 = \frac{U-J}{2}(N-1)^2 + \frac{U+3J}{2}(N-1) \approx 2U(N-1), \tag{3.12d}$$

$$E_5 = \frac{U-J}{2}N^2 + \frac{3}{2}(U+J)N - J \approx 3UN - U, \tag{3.12e}$$

and so on.

The order of the energies is

$$E_2 < E_1 < E_4 < E_3 < E_5 < \cdots . \tag{3.13}$$

The probability to find the state $|s\rangle$ contains the Boltzman factor $\exp(-E_s/k_{\rm B}T)$. Hence, the most dominant Markov chain consists only of the states $|1\rangle$ and $|2\rangle$, and it is denoted as $(1 \leftrightarrow 2)$. This process yields the spin-up current. We consider the second dominant process. Though $E_4 < E_3$, the state $|4\rangle$ can only be reached via the state $|3\rangle$, as illustrated in Fig.2. Namely, the second dominant chain is $(1 \leftrightarrow 2 \leftrightarrow 3 \leftrightarrow 4)$, which allows the spin-down current as well as the spin-up current.

First we analyze the most dominant process, which involves only the ground state and the first excited state (Fig.2). The currents are given by

$$I_\uparrow = \frac{I_0}{2}\left[f_{\rm L}(E_1 - E_2) - f_{\rm R}(E_1 - E_2)\right] = \frac{I_0}{2}\frac{\sinh(\Delta\mu/k_{\rm B}T)}{\cosh(\Delta\mu/k_{\rm B}T) + \cosh((U-\mu)/k_{\rm B}T)}, \tag{3.14a}$$

$$I_\downarrow = 0, \tag{3.14b}$$

where

$$I_0 = \frac{e\Gamma_{\rm L}\Gamma_{\rm R}}{\Gamma_{\rm L} + \Gamma_{\rm R}} \tag{3.15}$$

in terms of the tunneling rate Γ_χ given by (3.8).

The above expression can be further simplified in the following two limits. In the high-temperature limit ($\mu, \Delta\mu \ll k_{\rm B}T$) the sequential tunneling current takes a simple form

$$I_\uparrow \simeq \frac{I_0}{2}\Delta\mu \lim_{\Delta\mu\to 0}\frac{\partial f_{\rm L}(E_1 - E_2)}{\partial \Delta\mu} = I_0 \frac{\Delta\mu}{8k_{\rm B}T}\cosh^{-2}\left[\frac{\Delta_{12} - \mu}{2k_{\rm B}T}\right], \tag{3.16}$$

where $\Delta_{s's}$ is defined in (3.7). On the other hand, in the low-temperature limit ($k_{\rm B}T \ll \mu, \Delta\mu$) the current is given by

$$I_\uparrow = \frac{I_0}{2}\left[\theta(\mu_L - \Delta_{12}) - \theta(\mu_R - \Delta_{12})\right] \tag{3.17}$$

with the step function

$$\theta(x) = \begin{cases} 1, & x > 0 \\ 0, & x < 0 \end{cases}. \tag{3.18}$$

The current $I_\uparrow$ flows in the triangle domain ($\mu_L > \Delta_{12} > \mu_R$) in the $(\Delta\mu, \mu)$ plain.

In order to search for the down-spin polarized current $I_\downarrow$, it is necessary to analyze the second dominant process. It includes four states $(1 \leftrightarrow 2 \leftrightarrow 3 \leftrightarrow 4)$, as shown in the Fig.2. In this approximation, the transition matrix becomes a tridiagonal matrix, and we can solve the master equations exactly. The nonequilibrium density of states is calculated as

$$\rho_s = \frac{\widetilde{\rho}_s}{{\rm Tr}\widetilde{\rho}_s}, \qquad \widetilde{\rho}_s = \prod_{i=1}^{s-1}\frac{W(i+1,i)}{W(i,i+1)}, \tag{3.19}$$

where the index $s = 1, 2, 3, 4$ stands for the four states with the energy E_s. We can explicitly calculate $\widetilde{\rho}_s$ as

$$\widetilde{\rho}_s = e^{-\beta\widetilde{E}_s}\prod_{i=1}^{s-1}\frac{e^{\beta\widetilde{E}_i} + e^{\beta\widetilde{E}_{i+1}}\cosh\Delta\mu}{e^{\beta\widetilde{E}_i}\cosh\Delta\mu + e^{\beta\widetilde{E}_{i+1}}}, \tag{3.20}$$

with $\widetilde{E}_s = E_s - \mu n_{\rm tot}$. The current I_σ is calculable with the use of (3.10) and (3.4), whose result we show in the Fig.3. In particular we have

$$I_\downarrow = \frac{I_0}{4}\left[\theta(\mu_L - \Delta_{12}) - \theta(\mu_R - \Delta_{12})\right] \times \left[\theta(\mu_L - \Delta_{32}) - \theta(\mu_R - \Delta_{32})\right] \tag{3.21}$$

in the zero-temperature limit. The current $I_\downarrow$ flows in the triangle domain ($\mu_L > \Delta_{12} > \mu_R$ and $\mu_L > \Delta_{32} > \mu_R$) in the $(\Delta\mu, \mu)$ plain.

IV. FINITE-SIZE EFFECTS: REACTION TO QUASI-FERROMAGNET

In the conventional spin filter the ferromagnet is very rigid. On the other hand, the life time is finite in the case of a nanodisk, though it is quite long in spite of its small size. We

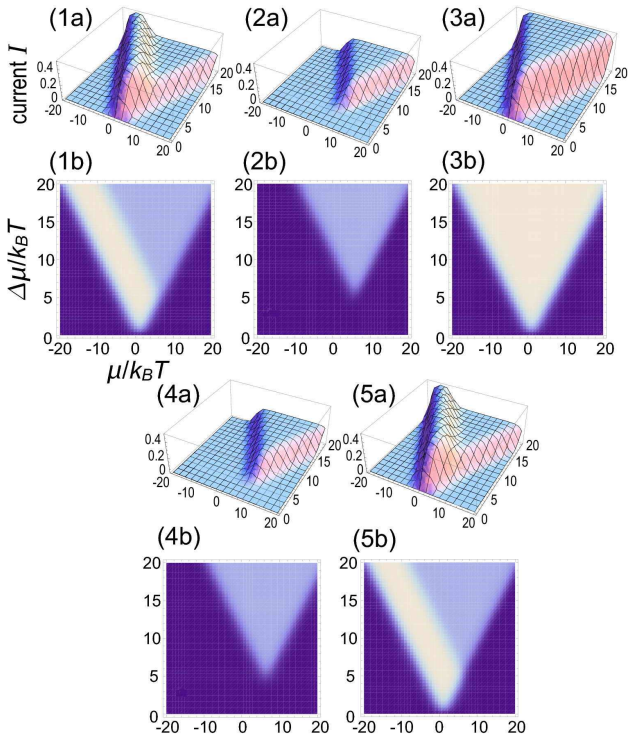

FIG. 3: Spin-dependent currents against $\mu/k_{\rm B}T$ and $\Delta\mu/k_{\rm B}T$ in the $N = 10$ nanodisk. We have set $U/k_{\rm B}T = 1$. The horizontal x-axis is the chemical potential $\mu/k_{\rm B}T$, and the horizontal y-axis is the bias voltage $\Delta\mu/k_{\rm B}T$. (a) The vertical z-axis is the current. (b) More currents flow in brighter regions. (1) The current I_1 induced by the process $1 \leftrightarrow 2$, which produces the up-spin polarized current. (2) The current I_2 induced by the process $3 \leftrightarrow 4$, which produces the up-spin polarized current. (3) The sum of the above two processes; $I_\uparrow = I_1 + I_2$. (4) The current I_4 induced by the process $2 \leftrightarrow 3$, which produces the down-spin polarized current; $I_\downarrow = I_4$. (5) The difference ΔI between the up-spin and down-spin current, $\Delta I = I_\uparrow - I_\downarrow = I_1 + I_2 - I_4$.

expect a reaction to the nanodisk spin from the spin-polarized current, provided the nanodisk spin is not controlled externally, say, by magnetic field. This effect is very interesting, since it is an intrinsic nature to quasi-ferromagnets.

We inject an electron into a nanodisk. Let $\Delta_{\uparrow\uparrow}$ or $\Delta_{\uparrow\downarrow}$ be the energy increase when the spin of an injected electron is parallel or anti-parallel to the nanodisk spin. According to the Hamiltonian (2.7) they are

$$\begin{aligned} \Delta_{\uparrow\uparrow} &= \Delta_{21} = -U, \\ \Delta_{\uparrow\downarrow} &= \Delta_{31} = UN. \end{aligned} \tag{4.1}$$

When the direction between the nanodisk spin and the electron spin is θ, the energy increase is given by

$$\langle H_{\rm D}^{\rm eff}\rangle = \Delta_{\uparrow\uparrow}\cos\frac{\theta}{2}\langle c_\uparrow^\dagger c_\uparrow\rangle + \Delta_{\uparrow\downarrow}\sin\frac{\theta}{2}\langle c_\downarrow^\dagger c_\downarrow\rangle, \tag{4.2}$$

where $\left\langle c_\sigma^\dagger c_\sigma\right\rangle$ represents the probability of finding the injected electron to have spin σ.

Based on the spin-rotational symmetry we may write the effective Hamiltonian as

$$H_{\rm D}^{\rm eff} = -J_{\rm sd}\boldsymbol{S}\cdot c^\dagger\boldsymbol{\sigma}c = -M\boldsymbol{n}\cdot c^\dagger\boldsymbol{\sigma}c, \tag{4.3}$$

where

$$J_{\rm sd} = MS_{\rm tot} = \Delta_{\uparrow\downarrow} - \Delta_{\uparrow\uparrow} = U\left(N+1\right), \tag{4.4}$$

and $\boldsymbol{n} = \boldsymbol{S}_{\rm tot}/S_{\rm tot}$ is the normalized spin with $S_{\rm tot} = |\boldsymbol{S}_{\rm tot}|$.

We introduce the Gilbert damping term phenomenologically,

$$H_\alpha = \alpha\dot{\boldsymbol{n}}^2, \tag{4.5}$$

where α is a dimensionless constant ($\alpha \approx 0.01$). Using the variational method for the Hamiltonian $H_{\rm D}^{\rm eff} + H_\alpha$, we obtain the Landau-Lifshitz-Gilbert equation,

$$\frac{\partial\boldsymbol{n}}{\partial t} = \gamma\boldsymbol{B}_{\rm eff}\times\boldsymbol{n} - \alpha\boldsymbol{n}\times\frac{\partial\boldsymbol{n}}{\partial t}, \tag{4.6}$$

where $\boldsymbol{B}_{\rm eff}$ is the effective magnetic field produced by the injected electron spin,

$$\gamma\boldsymbol{B}_{\rm eff} = \frac{1}{\hbar S_{\rm tot}}\left\langle\frac{\partial H_{\rm D}^{\rm eff}}{\partial\boldsymbol{n}}\right\rangle = -\frac{M}{\hbar S_{\rm tot}}\left\langle c^\dagger\boldsymbol{\sigma}c\right\rangle, \tag{4.7}$$

with the gyromagnetic ratio γ.

For definiteness we now inject the up-spin electron to the nanodisk. The effective magnetic field is

$$\gamma\boldsymbol{B}_{\rm eff} = (0,0,\gamma B_{\rm eff}) = -\frac{M}{\hbar S_{\rm tot}}\left\langle c^\dagger\boldsymbol{\sigma}c\right\rangle. \tag{4.8}$$

We investigate the dynamics of the normalized spin $\boldsymbol{n}$ of the nanodisk under this field. In the polar coordinate, setting

$$\boldsymbol{n} = (\sin\theta\cos\phi, \sin\theta\sin\phi, \cos\theta), \tag{4.9}$$

we rewrite the Landau-Lifshitz-Gilbert equation (4.6) as

$$\dot\theta = \alpha\dot\phi\sin\theta, \qquad \dot\phi\sin\theta = \gamma B_{\rm eff}\sin\theta - \alpha\dot\theta. \tag{4.10}$$

This is equivalent to

$$\dot\theta = \frac{\alpha\gamma B_{\rm eff}}{1+\alpha^2}\sin\theta, \qquad \dot\phi = \frac{\gamma B_{\rm eff}}{1+\alpha^2}, \tag{4.11}$$

which we can solve explicitly,

$$\begin{aligned} \theta\left(t\right) &= 2\tan^{-1}\exp\left[-\left(t-t_0\right)/\tau_{\rm filter}\right], \\ \phi\left(t\right) &= \frac{\gamma B_{\rm eff}}{1+\alpha^2}t, \end{aligned} \tag{4.12}$$

where t_0 is an integration constant, and $\tau_{\rm filter}$ is the relaxation time given by

$$\tau_{\rm filter} = \frac{1+\alpha^2}{2\alpha\gamma\left|B_{\rm eff}\right|} \propto N. \tag{4.13}$$

It is proportional to $S_{\rm tot}/M$ and hence proportional to the disk size N because of (4.7). The initial phase θ_0 is related to the parameter t_0 as

$$\theta\left(0\right) = 2\tan^{-1}\exp\left[t_0/\tau_{\rm filter}\right]. \tag{4.14}$$

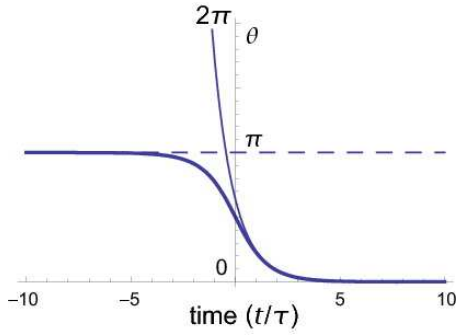

FIG. 4: The bold curve is the relaxation process of spin in nanodisk. The horizontal axis is the time t/τ and the vertical axis is the angle θ. The thin curve is the asymptotic function $\theta = 2\exp\left[-\left(t-t_0\right)/\tau_{\text{filter}}\right]$ of the bold curve for $t \gg t_0$. The dotted line is the asymptotic value for $t \ll t_0$.

Thus, $t_0 = 0$ corresponds to

$$\theta\left(0\right) = \frac{\pi}{2}. \tag{4.15}$$

We use the parameter t_0 instead of the initial phase $\theta\left(0\right)$ for simplicity.

The time scale for the direction of the nanodisk spin to align with that of the spin-polarized current is τ_{filter}, where the effective magnetic field (4.7) is proportional to the injected current I^{in}. In other words, we can control the polarization of the nanodisk spin by using the spin-polarized current. We note that this is possible since the nanodisk is a quasi-ferromagnet. Indeed, there exist no effective magnetic field (4.7) in the conventional ferromagnet.

V. SPINTRONIC DEVICES AND APPLICATIONS

We summarize the spin properties of a nanodisk and an incoming electric current. First of all, being a quasi-ferromagnet, the nanodisk has a definite polarization. With respect to the incoming electric current there are three cases. (1) The polarized current, where all electrons have a definite polarization, rotates the nanodisk spin to that of the incoming current, as we have shown in Sec.IV. (2) The unpolarized current, where the polarization of each electron is completely random, does not induce any effective magnetic field. Hence it is filtered so that the outgoing current is polarized to that of the nanodisk. (3) The partially polarized current, where the polarization of each electron is at random but the averaged polarization has a definite direction, induces a net effective magnetic field. Hence it rotates the nanodisk spin to that of the incoming current, and then is filtered so that the outgoing current is completely polarized to the averaged polarization of the incoming current. Furthermore, it is possible to control the nanodisk spin externally by applying magnetic field. Then the outgoing current has the same polarization as that of the nanodisk, irrespective of the type of incoming current. Using these properties we propose some applications of graphene nanodisks for spintronic devices.

A. Spin Memory

The first example is a spin memory.[8] For a good memory device three conditions are necessary: (i) It keeps a long life time information; (ii) Information stored in the memory can be read out without changing the information stored; (iii) It is possible to change the information arbitrarily.

First, since the life time of the nanodisk quasi-ferromagnet is very long compared to the size[14],

$$\tau_{\text{ferro}} \propto N^2, \tag{5.1}$$

we may use the nanodisk spin as an information. Next, we can read-out this information by applying a spin-unpolarized current. The outgoing current from a nanodisk is spin-polarized to the direction of the nanodisk spin. Thus we can obtain the information of the nanodisk spin by observing the outgoing current. Finally, the direction of the nanodisk spin can be controlled by applying a spin-polarized current into the nanodisk.

Thus, the nanodisk spin satisfies the conditions as a memory device. The important point is that the size is of the order of nanometer, and it is suitable as a nanodevice.

B. Spin Amplifier

The second example is a spin amplifier. We inject a partially-polarized-spin current, whose average direction we take to be up for definiteness. Thus, $I_{\uparrow}^{\text{in}} > I_{\downarrow}^{\text{in}} > 0$. On the other hand, the direction of the nanodisk spin is arbitrary. Since spins in the nanodisk feel an effective magnetic field proportional to $I_{\uparrow}^{\text{in}} - I_{\downarrow}^{\text{in}}$, they are forced to align with that of the partially-polarized-spin current after making damped precession. By using (4.12) the time dependence is given by

$$I_{\uparrow}\left(t\right) = I_{\uparrow}^{\text{in}} \cos\frac{\theta\left(t\right)}{2} = I_{\uparrow}^{\text{in}} \frac{1}{\sqrt{1+\exp\left[-2t/\tau_{\text{filter}}\right]}}, \tag{5.2a}$$

$$I_{\downarrow}\left(t\right) = I_{\downarrow}^{\text{in}} \sin\frac{\theta\left(t\right)}{2} = I_{\downarrow}^{\text{in}} \frac{1}{\sqrt{1+\exp\left[2t/\tau_{\text{filter}}\right]}}, \tag{5.2b}$$

where we have set $t_0 = 0$, which means $\theta\left(0\right) = \pi/2$: See Fig.5. The outgoing current is initially given by

$$I_{\uparrow}\left(0\right) = \frac{1}{\sqrt{2}} I_{\uparrow}^{\text{in}}, \qquad I_{\downarrow}\left(0\right) = \frac{1}{\sqrt{2}} I_{\downarrow}^{\text{in}}. \tag{5.3}$$

as a function of the incoming current I_{σ}^{in}. The time scale is given by the relaxation time (4.13).

After enough time $t - t_0 \gg \tau$, all spins in the nanodisk take the up direction and hence the outgoing current $I_{\sigma}^{\text{out}} \equiv \lim_{t\to\infty} I_{\sigma}\left(t\right)$ is the perfectly up-polarized one,

$$I_{\uparrow}^{\text{out}} = I_{\uparrow}^{\text{in}}, \qquad I_{\downarrow}^{\text{out}} = 0. \tag{5.4}$$

Consequently, the small difference $I_{\uparrow}^{\text{in}} - I_{\downarrow}^{\text{in}}$ is amplified to the large current $I_{\uparrow}^{\text{in}}$. The amplification ratio is given by $I_{\uparrow}^{\text{in}}/(I_{\uparrow}^{\text{in}} - I_{\downarrow}^{\text{in}})$, which can be very large. This effect is very important because the signal of spin will easily suffer from damping by disturbing noise in leads. By amplifying the signal we can make circuits which are strong against noises.

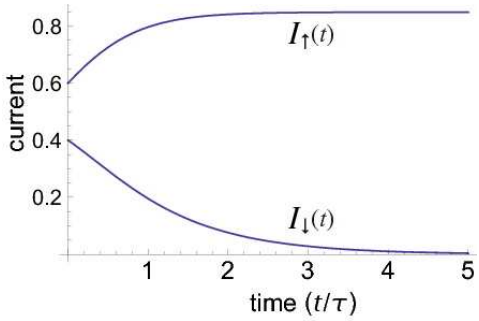

FIG. 5: Relaxation process of spin amplifier. The horizontal axis is the time t/τ and the vertical axis is the current $I_\uparrow$ and $I_\downarrow$. We have set $I_\uparrow^{\rm in} = 0.6\sqrt{2}$, $I_\downarrow^{\rm in} = 0.4\sqrt{2}$. The currents saturate after enough time ($t \gtrsim 2\tau$ for $I_\uparrow$, $t \gtrsim 5\tau$ for $I_\downarrow$), and the amplification ratio is 3 in this example.

C. Spin Valve and Spin-Field-Effect Transistor

The third example is a spin valve, or giant magnetoresistance effect [Fig.6].[39,40,41] We set up a system composed of two nanodisks sequentially connected with leads. We apply external magnetic field, and control the spin direction of the first nanodisk to be

$$|\theta\rangle = \cos\frac{\theta}{2}|\uparrow\rangle + \sin\frac{\theta}{2}|\downarrow\rangle\,, \tag{5.5}$$

and that of the second nanodisk to be

$$|0\rangle = |\uparrow\rangle\,. \tag{5.6}$$

We inject an unpolarized-spin current to the first nanodisk. The spin of the lead between the two nanodisks is polarized into the direction of $|\theta\rangle$. Subsequently the current is filtered to the up-spin one by the second nanodisk. The outgoing current from the second nanodisk is

$$I_\uparrow^{\rm out} = I_\uparrow \cos\frac{\theta}{2}. \tag{5.7}$$

Since we can arrange the angle θ externally, we can control the magnitude of the up-polarized current from zero to one. In this sense the system act as a spin valve.

The forth example is a spin-field-effect transistor[36] [Fig.7]. We again set up a system composed of two nanodisks sequentially connected with leads. We now apply the same external magnetic field to both these nanodisks, and fix their spin direction to be up,

$$|0\rangle = |\uparrow\rangle\,. \tag{5.8}$$

As an additional setting, we use a lead between the two nanodisks possessing a strong Rashba-type spin-orbit coupling[37],

$$H_{\rm R} = \frac{\lambda}{\hbar}\left(p_x\sigma^y - p_y\sigma^x\right). \tag{5.9}$$

Spins make precession while they pass through the lead. The spin-rotation angle is given by[4]

$$\Delta\theta = 2\lambda m^* L/\hbar, \tag{5.10}$$

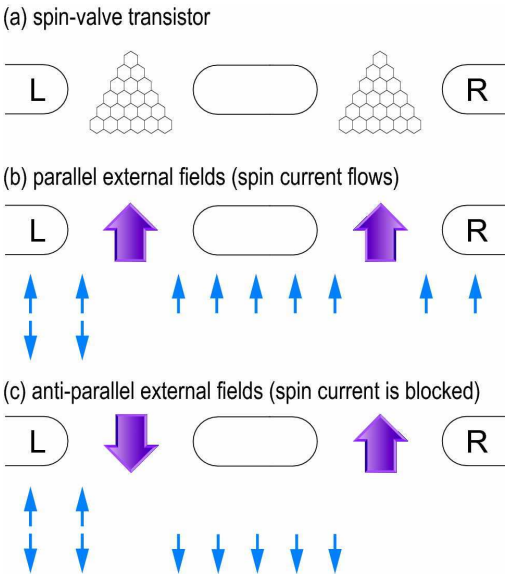

FIG. 6: Illustration of spin valve with unpolarized current incoming from left. Spins of each nanodisk are controled by the external magnetic field. The unpolarized current is filtered by the left nanodisk, and only electrons whose spin direction is the same as the nanodisk spin go through the centeral lead. (a) The spin valve is made of two nanodisks with the same size, which are connected with leads. (b) We apply the external magnetic field in the same direction. The spin-polarized outgoing current flows. (c) We apply the external magnetic field in the opposite directions. The outgoing current is blocked.

where m^* is the electron effective mass in the lead and L is the length of the lead. We can control $\Delta\theta$ by changing the coupling strength λ externally by applying electric field.[42] The outgoing current from the second nanodisk is

$$I_\uparrow^{\rm out} = I_\uparrow \cos\frac{\Delta\theta}{2}. \tag{5.11}$$

Since we can arrange the angle $\Delta\theta$ by applying electric field and control the magnitude of the up-polarized current from zero to one, we expect the system acts as a spin-field-effect transistor as in the conventional case.

D. Spin Diode

The fifth example is a spin diode [Fig.8]. We use a system similar to the spin-field-effect transistor but with the following differences. First, two nanodisks have different sizes. When the left nanodisk is larger than the right nanodisk, the relaxation time of the left nanodisk $\tau_{\rm L}(\equiv \tau_{\rm filter}^{\rm L})$ is larger than that of the right nanodisk $\tau_{\rm R}(\equiv \tau_{\rm filter}^{\rm R})$,

$$\tau_{\rm L} > \tau_{\rm R}. \tag{5.12}$$

Second, the applied magnetic field is taken so small that the nanodisk spin can be controlled by a polarized current. For definiteness we take the direction of the magnetic field to be up. Third, the lead has the Rashba-type interaction such that

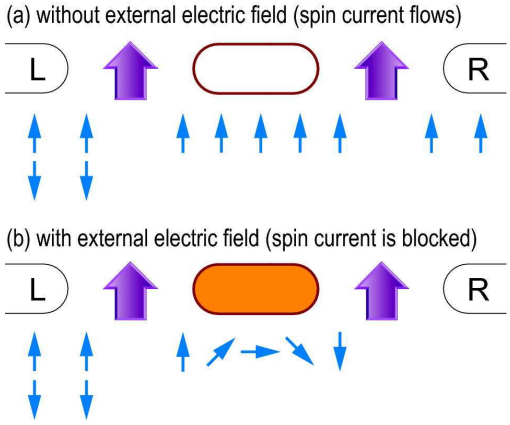

FIG. 7: Illustration of spin-field-effect transistor with unpolarized current coming from left. We apply the same external magnetic field to both of the nanodisks. The unpolarized current is filtered by the left nanodisk, and only up-spin electrons go through the centeral lead. (a) Without external electric field, the electron spin in the central lead does not rotate, and the outgoing spin-polarized current exists. (b) With an appropriate external electric field, since the electron spin in the central lead rotates by the Rashba-type interaction, the outgoing current does not exist.

the rotation angle is $\Delta\theta = \pi - \delta$ with small δ, say, $\delta \simeq 0.1\pi$. When no currents enter the nanodisk, the direction of two nanodisk spins is identical due to a tiny external magnetic field. When we inject the current in this state, the net outgoing current is very small,

$$I^{\text{out}} = \cos\frac{\pi-\delta}{2} \simeq 0. \tag{5.13}$$

This is the "off" state of spin diode.

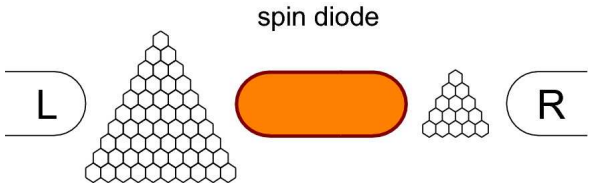

FIG. 8: Illustration of spin diode made of two nanodisks with different size. By controlling the bias voltage $\Delta\mu$, the current flows from the left lead to the right lead ($\Delta\mu > 0$), or in the opposite way ($\Delta\mu < 0$). The incoming current is unpolarized, which is made polarized by the first nanodisk. The electron spin in the central lead is rotated by the Rashba-type interaction.

Let us inject an unpolarized pulse square current to the system, starting at $t = t_i$ and finishing at $t = t_f$,

$$I_\sigma(t) = I^{\text{in}}\theta(t-t_i)\theta(t_f-t), \tag{5.14}$$

where σ denotes the spin. The system become the "on" state by the pulse. When the bias voltage is such that $\Delta\mu > 0$, the current flows into the left nanodisk and then into the right nanodisk. The left nanodisk acts as a spin filter. The current in the central lead is initially up-polarized but is rotated by the angle $\Delta\theta$ due to the Rashba-type coupling effect. Then it enters the right nanodisk. Since the relaxation time is τ_{R}, the total spin-dependent charge carried by the current is given by

$$Q_\uparrow = \int_{t_i}^{t_f} I_\uparrow dt = Q_\uparrow(t_f) - Q_\uparrow(t_i), \tag{5.15a}$$

$$Q_\downarrow = \int_{t_i}^{t_f} I_\downarrow dt = Q_\downarrow(t_f) - Q_\downarrow(t_i) \tag{5.15b}$$

with

$$Q_\uparrow(t) = I^{\text{in}}\tau_{\text{R}}\sinh^{-1}\left[\exp\left[(t-t_0)/\tau_{\text{R}}\right]\right], \tag{5.16a}$$

$$Q_\downarrow(t) = I^{\text{in}}\tau_{\text{R}}\sinh^{-1}\left[\exp\left[-(t-t_0)/\tau_{\text{R}}\right]\right]. \tag{5.16b}$$

On the other hand, when $\Delta\mu < 0$, the current enter the right nanodisk and goes out from the left nanodisk. Since the relaxation time is τ_{L}, the total spin-dependent charge is given by the above formulas but with the replacement of τ_{R} by τ_{L}. Because the size of two nanodisk are different, these two currents behave in a different way.

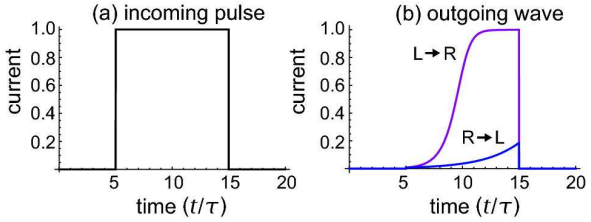

FIG. 9: Pulse wave. The horizontal axis is the time and the vertical axis is the current. (a) The incoming pulse wave. (b) The outgoing waves for $L \to R$ and $R \to L$. They are very different for the same incoming pulse wave due to the difference in the nanodisk size. We have set $t_i = 5, t_f = 15$, and $\tau_{\text{L}} = 3\tau_{\text{R}}$.

We define the direction dependent total charge $Q_\sigma(L \to R)$ and $Q_\sigma(R \to L)$, where $Q_\sigma(L \to R)$ is the total charge with the spin σ when charges flow from left to right, while $Q_\sigma(R \to L)$ is the total charge when charges flow from right to left. We find the relation

$$Q_\uparrow(L \to R) > Q_\uparrow(R \to L) \gg Q_\downarrow(R \to L) > Q_\downarrow(L \to R) \tag{5.17}$$

from (5.12), which implies the up (down) component increases (decreases) from the initial value.

We define the rectification coefficient by

$$R = \frac{Q_\uparrow(L \to R) + Q_\downarrow(L \to R)}{Q_\uparrow(R \to L) + Q_\downarrow(R \to L)}, \tag{5.18}$$

which is approximately equals to

$$R \simeq \frac{Q_\uparrow(L \to R)}{Q_\uparrow(R \to L)}. \tag{5.19}$$

We illustrate this rectification coefficient as a function of the pulse width $\Delta t = t_f - t_i$ for various initial phases $\theta(0)$ or equivalently t_0 in Fig.10. Each curve has a peak structure. Hence, when the relaxation-time ratio $\tau_{\text{L}}/\tau_{\text{R}}$ and the initial

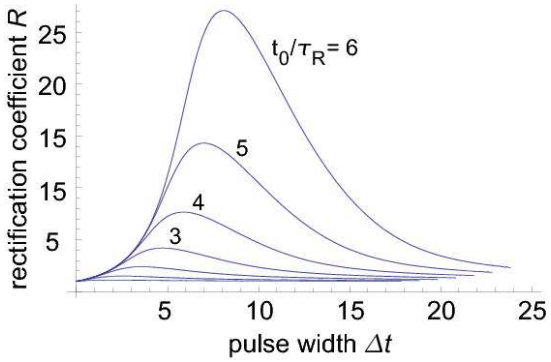

FIG. 10: The vertical axis is the rectification coefficient R. The horizontal axis is the pulse width $\Delta t = t_f - t_i$. We plot R for various initial values $t_0/\tau_{\rm R} = \log\tan\left[(\pi-\delta)/2\right]$. We have set $\tau_{\rm L} = 3\tau_{\rm R}$.

phase $\theta\,(0)$ are given, it is possible to optimize the width Δt so that the rectification coefficient R is maximized. This maximized value of R diverges as $\theta\,(0) \to \pi$. However, the relaxation time diverges as well. It would be efficient to take the initial phase $\theta\,(0)$ to make $t_0/\tau_{\rm R} \simeq 5$ for a spin diode.

VI. CONCLUSIONS

We have studied the electromagnetic properties of the zigzag trigonal nanodisk by projecting the system to the zero-energy sector. We may regard it as a quasi-ferromagnet characterized by the exchange energy as large as the Coulomb energy. The system is well approximated by the SU(N) Heisenberg-Hubbard model. The relaxation time is finite but quite large even if the size is very small. Being a ferromagnet, it can be used as a spin filter. Namely, only electrons with spin parallel to the spin of the nanodisk can go through it. Additionally, it has a novel feature that it is not a rigid ferromagnet. The incoming spin-polarized current can rotate the nanodisk spin itself. Combining the advantages of both these properties, we have proposed a rich variety of spintronic devices, such as spin memory, spin amplifier, spin valve, spin-field-effect transistor and spin diode. Graphene nanodisks could well be basic components of future nanoelectronic and spintronic devices.

I am very much grateful to N. Nagaosa and S. Tarucha for many fruitful discussions on the subject.

[1] S. Murakami, N. Nagaosa, S.-C. Zhang, Science **301**, 1348 (2003).
[2] Y. Ohno, D. K. Young, B. Beschoten, F. Matsukura, H. Ohno and D. D. Awschalom, Nature **402**, 790 (1999).
[3] See, e.g., Realizing Controllable Quantum States: Mesoscopic Superconductivity and Spintronics, edited by H. Takayanagi and J. Nitta, World Scientific, Singapore, 2005, and references therein.
[4] I. Zŭtić, J. Fabian and S. Das Sarma, Rev. Mod. Phys., **76**, (2004), and references therin.
[5] S. A. Wolf, D. D. Awschalom, R. A. Buhrman, J. M. Daughton, S. von Molnár, M.L.Roukes, A. Y. Chtchelkanova and D. M. Treger, Science **294**, 1488 (2001), and references therin.
[6] G. A. Prinz, Science **282**, 1660 (1998), and references therin.
[7] H. Akinaga and H. Ohno, IEEE Transactions on nanotechnology **1**, 19 (2002).
[8] P. Recher, E. V. Sukhorukov and D. Loss, Phys. Rev. Lett., **85**, 1962 (2000).
[9] J. A. Folk, R. M. Potok, C. M. Marcus and V. Umansky, Science **299**, 679 (2003).
[10] N. Tombros, C. Jozsa, M. Popinciuc, H. T. Jonkman, B. J. van Wees, Nature **448**, 571 (2007).
[11] V. M. Karpan, G. Giovannetti, P. A. Khomyakov, M. Talanana, A. A. Starikov, M. Zwierzycki, J. van den Brink, G. Brocks, P. J. Kelly, Phys Rev Lett **99**, 176602 (2007).
[12] L.Brey, H.A.Fertig, Phys. Rev. B **76**, 205435 (2007).
[13] M. Ezawa, Physica Status Solidi (c) **4**, No.2, 489 (2007).
[14] M. Ezawa, Phys. Rev. B **76**, 245415 (2007): M. Ezawa, Physica E **40**, 1421-1423 (2008).
[15] J. Fernández-Rossier, and J. J. Palacios, Phys. Rev. Lett. **99**, 177204 (2007).
[16] O. Hod, V. Barone, and G. E. Scuseria, Phys. Rev. B 77, 035411 (2008).
[17] M. Ezawa, Phys. Rev. B **77**, 155411 (2008).
[18] K. S. Novoselov, A. K. Geim, S. V. Morozov, D. Jiang, Y. Zhang, S. V. Dubonos, I. V. Grigorieva, and A. A. Firsov, Science **306**, 666 (2004).
[19] K. S. Novoselov, A. K. Geim, S. V. Morozov, D. Jiang, M. I. Katsnelson, I. V. Grigorieva, S. V. Dubonos, and A. A. Firsov, Nature **438**, 197 (2005).
[20] Y. Zhang, Y. -W Tan, H. L. Stormer, and P. Kim, Nature **438**, 201 (2005).
[21] M. Fujita, K. Wakabayashi, K. Nakada, and K. Kusakabe, J. Phys. Soc. Jpn. **65**, 1920 (1996).
[22] M. Ezawa, Phys. Rev. B, **73**, 045432 (2006).
[23] L. Brey, and H. A. Fertig, Phys. Rev. B, **73**, 235411 (2006).
[24] F. Muñoz-Rojas, D. Jacob, J. Fernández-Rossier, and J. J. Palacios, Phys. Rev. B, **74**, 195417 (2006).
[25] Y. -W Son, M. L. Cohen, and S. G. Louie, Phys. Rev. Lett., **97**, 216803 (2006).
[26] V. Barone, O. Hod, and G. E. Scuseria, Nano Lett., **6**, 2748 (2006).
[27] M. Y. Han, B. Oezyilmaz, Y. Zhang, and P. Kim, Phys. Rev. Lett., **98**, 206805 (2007).
[28] Z. Chen, Y. -M. Lin, M. J. Rooks, and P. Avouris, Physica E, **40**, 228 (2007).
[29] Z. Xu and Q. -S. Zheng, Appl. Phys. Lett. **90**, 223115 (2007).
[30] B. Özyilmaz, P. Jarillo-Herrero, D. Efetov and P. Kim, Appl. Phys. Lett. **91**, 192107 (2007).
[31] C. Berger, Z. Song, X. Li, X. Wu, N. Brown, C. Naud, D. Mayou, T. Li, J. Hass, A.N. Marchenkov, E. H. Conrad, P.N. First and W. A. de Heer, Science **312**, 119 (2006).
[32] H. J. Räder, A. Rouhanipour, A. M. Talarico, V. Palermo, P. Samorì, and K. Müllen, Nature materials **5**, 276 (2006).
[33] W. G. van der Wiel, S. De Franceschi, J. M. Elzerman, T. Fujisawa, S. Tarucha and L. P. Kouwenhoven, Rev. Mod. Phys. **75**, 1 (2003).
[34] C.W.J. Beenakker, Phys. Rev. B **44**, 1646 (1991).
[35] V.y N. Golovach and D. Loss, Phys. Rev. B **69**, 245327 (2004).
[36] S. Datta and B. Das, Appl. Phys. Lett. **56**, 665 (1990).
[37] E. I. Rashba, Fiz. Tverd. Tela (Leningrad) **2**, 1224 (1960) [Sov. Phys. Solid State **2**, 1109 (1960)]; Y. A. Bychkov and E. I. Rashba,

J. Phys. C **17**, 6039 (1984).
[38] T. Koga, J. Nitta, H. Takayanagi and S. Datta, Phys. Rev. Lett. **88**, 126601 (2002).
[39] M. N. Baibich, J. M. Brot, A. Fert, N. V. Dau and F. Petroff, Phys. Rev. Lett. **61**, 2472 (1988).
[40] G. Binasch, P. Grunberg, F. Saurenbach and W. Zinn, Phys. Rev. B **39**, 4828 (1989).
[41] Y. M. Lee, J. Hayakawa, S. Ikeda, F. Matsukura and H. Ohno, Appl. Phys. Lett. **90**, 212507 (2007).
[42] J. Nitta, T. Akazaki, and H. Takayanagi, Phys. Rev. Lett. **78**, 1335 (1997).